© 2014, Scienceline Publication
www.science-line.com
ISSN: 2322-5114
Journal of World's Electrical Engineering and Technology
J. World. Elect. Eng. Tech. 3(2): 89-92, 2014
JWEET

Semi-supervised Discriminant Analysis for Skin Detection in Color Images

Peyman Mobini

Department of Electrical and Electronic Engineering, Islamic Azad University, Bonab Branch, Iran
Corresponding author's Email: peyman.mobini.1989@gmail.com

ORIGINAL ARTICLE
Received 10 May. 2014
Accepted 20 Aug. 2014

Abstract *– A new algorithm for skin segmentation in color images is presented in this paper based on semi-supervised discriminant analysis (SDA). At first, input RGB space input image is transferred to YC_bC_r and CIE Lab color space in which skin pixels are more similar to each other and different from pixels of other objects. Some components of new color spaces are treated as features of pixels and construct feature vectors. Feature vectors are given to SDA algorithm to decrease the inter-class distances and increase between-class distances. Finally, projected vectors are given to the K-nearest neighbor (KNN) classifier to separate skin pixels from non-skin pixels. Simulation results show that proposed approach has considerable efficiency in skin pixel detection.*

Keywords*: KNN, Lab, SDA, skin, YC_bC_r*

INTRODUCTION

The aim of skin detection is to find the location of the skin regions in an unconstrained input image. Skin detection is commonly used in order to determine pixels related to human skin, which is in important preprocessing in a large number of applications [1], such as face detection [2], face tracking, human motion analysis [3], hand segmentation for gesture analysis [4], and filtering of objectionable Web images [5, 6]. Detection of skin regions in these applications can reduce the search space for finding the interesting objects.

In [7], authors have used multi-layer perceptron (MLP) neural network to separate skin pixels from others. They examine different chromatic components of YC_bC_r color space as well as combination of them. Their results show that difference of C_b and C_r achieves the highest performance. Authors in [8] have presented as framework for sign language recognition. They firstly use support vector active learning and region segmentation to build skin model and then this model is integrated with the motion and position information to perform segmentation and tracking. Real Adaboost algorithm was used in [9] with set of LUT-type weak classifiers to describe the distribution chromatic components of YC_bC_r color space. Adaptive Bayesian decision theory was developed in [10] based on texture characteristics to skin segmentation. In [11], at first efficient 16-Gaussian Mixture Models (GMM) classifier was used for segmentation and then efficient features were extracted as Shannon entropy of 2-D Daubechies wavelet. Finally, K-means clustering algorithm was used to distinguish skin pixels from others.

In this paper, we present a new efficient algorithm for skin detection in color images. Input RGB color space image is transformed to YC_bC_r and *CIE Lab* color spaces. Then, C_b and C_r components from YC_bC_r color space, and *a* and *b* components from *CIE Lab* color space construct feature vectors. Due to abilities of semi-discriminant analysis (SDA) algorithm, these vectors are given to SDA to decrease the inter-class distances and increase between-class distances. In this paper, we face to binary classification problem, because each pixel belongs to skin or non-skin pixels. We choose K-nearest neighbor (KNN) classifier to distinguish skin pixels from non-skin pixels. In order to evaluate the efficiency of the proposed skin detector, we choose Compaq database [12]. Obtained results demonstrate that proposed skin detector has good ability in separating skin pixels from non-skin pixels.

Following this introduction, SDA, YC_bC_r and *CIE Lab* color spaces are briefly explained. Proposed skin-detector is presented in details in Section III. Simulation results are presented in Section IV and finally Section V concludes this paper.

PRELIMINARIES

Here, we explain briefly semi-supervised discriminant analysis (SDA), and color spaces used in this paper.

A. SDA

One of the most popular methods for extracting features which keep class separability is linear discriminant analysis (LDA). Maximizing the between-class covariance (S_b) and minimizing the within-class covariance (S_w) result in projected vectors. The problem arises when there are no sufficient training samples to obtain the covariance matrix of each class accurately. SDA is an efficient method proposed to overcome this problem. SDA uses both labeled and unlabeled. Labeled data points are used maximize separability between different classes as well as intrinsic geometrical structure obtained from both labeled and unlabeled data points [13].

B. YC_bC_r color space

Increasing demands for digital algorithms especially in digital video results in introducing YC_bC_r color space for handling video information [14]. YC_bC_r color space is obtained by weighted sum of RGB space components. In this space, luminance information is stored as a single component (Y), while chrominance information is stored in two components (C_b and C_r). C_b represents the difference between the blue component and a reference value as well as C_r represents the difference between the red component and a reference value [15]. Components of YC_bC_r color space are obtained as

$$Y = 65.481 \times R + 128.553 \times G + 24.996 \times B + 16 \quad (1)$$

$$C_b = -37.797 \times R - 74.203 \times G + 112 \times B + 128 \quad (2)$$

$$C_r = 112 \times R - 93.786 \times G - 18.214 \times B + 128 \quad (3)$$

where R, G, and B denote the red, green, and blue components of RGB color space respectively.

C. CIE Lab color space

CIE Lab color space is proposed by International Commission on Illumination (CIE) and has some properties of high importance like device-independency and perceptual linearity. CIE Lab color space is obtained from CIE XYZ color space. Perceptual distance between colors and approximate perceptual uniformity is normalized in this model. This property makes equal differences of colors in the color space should produce equally important color changes in human perception [16].

PROPOSED SKIN-DETECTOR

In this Section, we explain our proposed algorithm for skin detection in color images. The main steps of our proposed algorithm are as follows

- Use color space transformation to obtain efficient color space
- Construct feature vector
- Apply SDA
- Skin detection by KNN

In the following, these steps are explained in details.

A. Color space transformation

Input RGB space colored image must be transformed into the space in which skin pixels are highly separated from non-skin pixels. In other words, in new color spaces skin pixels should be similar to each other and different from non-skin pixels. In this paper, we use YC_bC_r and *Lab* color spaces in proposed skin-detector. Therefore, at first input image is transformed to YC_bC_r and *Lab* color spaces. A typical *RGB* image and its equivalent images in the YC_bC_r and *Lab* spaces are shown in Fig. 1.

B. Construct feature vector

Each of YC_bC_r and Lab color spaces has three components. From these components, we should choose those that can provide efficient separability between skin and non-skin pixels. In Fig. 2, components of these color spaces are shown. In C_b component, pixels are darker than the other pixels, i.e., skin pixels has low grayscale values in C_b component. In contrast to C_b component, in C_r component, skin pixels have high grayscale values and seem brighter. In Y component, there is no sensible difference between skin pixels and non-skin pixels. Therefore, C_b and C_r components can provide separate skin pixels form others, but Y component does not have this ability for separation. Hence, we can use C_b and C_r components as first and second features. From three components of *Lab* color space, only the component b can distinguish skin pixels from others and can be used as third feature and the other two components i.e., L and a cannot provide separability between skin and non-skin pixels. Based on mentioned explanations, feature vector in our proposed skin-detector has three dimension; C_b, C_r, and b.

In Fig. 3, the scatter plot of skin and non-skin pixels in 3-dimensional feature space is shown. It is observed that these three features i.e., C_b, C_r, and b, can provide relatively good separability as well as some non-skin pixels are fall in the area of skin pixels which degrades the performance of skin-detector system.

a b c

Fig. 1 – A typical image in different color spaces. (a) RGB, (b) YC_bC_r, (c) *Lab*

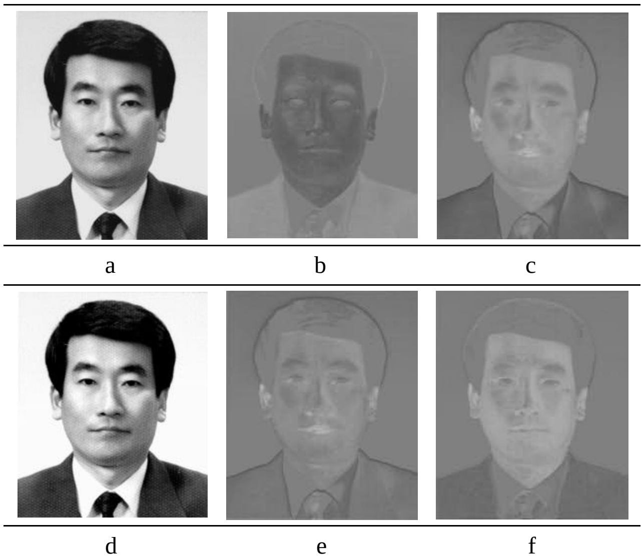

Fig. 2 – Components of YC_bC_r and *Lab* spaces, (a)-(c) Y, C_b, C_b of YC_bC_r, respectively; (d)-(e) L, a, b of *Lab*, respectively.

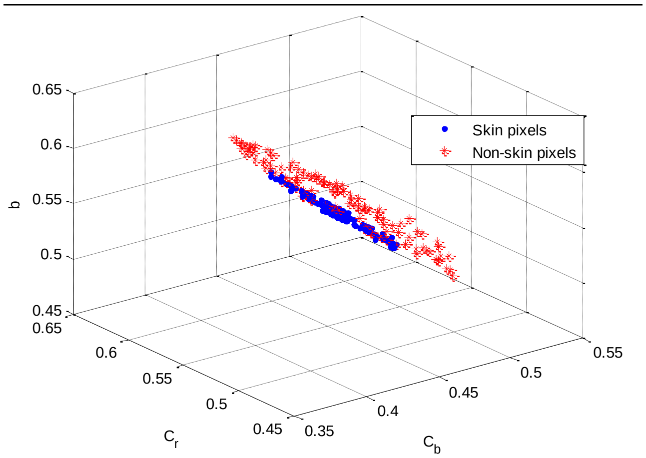

Fig. 3- scatter plot of skin and non-skin pixels in 3-dimensional feature space

C. Apply SDA

In order to enhance the separability between two classes, we propose to use SDA as a part of proposed skin-detector. As mentioned SDA uses labeled and unlabeled data points to decrease inter-class and increase between-class distances. Therefore, both labeled and unlabeled data points are given to SDA algorithm.

In addition to enhance the inter-class and between-class distances, SDA reduces the dimension of the feature vector given to it. If the dimension of the input feature vector is lower than the number of classes, SDA does not reduce the dimension of the input feature vector and the dimension of the output vector is the same as input vector. On the other side, if the dimension of input feature vector is higher than the number of classes, SDA reduces the dimension of input feature vector. In this case, the dimension of the output vector is equal to the number of classes. In our proposed, the dimension of input feature vector to SDA is three, and we have two classes. Therefore, the size of output feature vector is two. This reduction is done by keeping the two largest eigenvalues and removing the smaller one. In Fig. 4, the scatter plot of features obtained from SDA is shown in 2-dimensional feature space. As seen, the distances between skin and non-skin pixels are increased.

RESULTS

Here, we present the performance of the proposed skin-detector system. In order to evaluate the performance of the proposed algorithm, we use Compaq skin database [12]. We use three metrics to evaluate the performance of the proposed skin-detector; correct detection rate (CDR), false acceptance rate (FAR), and false rejection rate (FRR) that are defined as follows [7].

$$\mathrm{CDR} = \frac{\text{Number of pixels correctly classified}}{\text{Total pixels in the test database}} \tag{4}$$

$$\mathrm{FAR} = \frac{\text{Number of non-skin pixels classified as skin pixels}}{\text{Total pixels in the test database}} \tag{5}$$

$$\mathrm{FRR} = \frac{\text{Number of skin pixels classified as non-skin pixels}}{\text{Total pixels in the test database}} \tag{6}$$

From database, we choose 20000 pixels where half of them are skin pixels and the other half are non-skin pixels. 3000 pixels from each class are chosen as skin pixels and the remaining pixels are used in test phase.

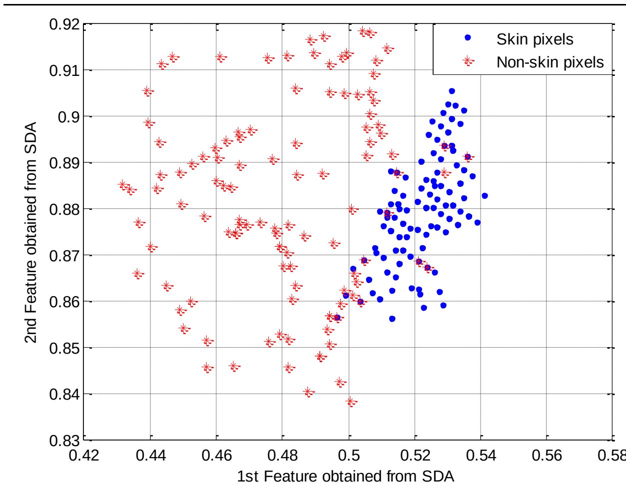

Fig. 4- Scatter plot of skin and non-skin pixels obtained from SDA in 2-dimensional feature space

In order to increase separability by SDA, 2000 pixels from each class are used as labeled data, and 1000 pixels from each class are used as unlabeled data.

Therefore, totally 6000 skin samples are used in training step and the remaining 14000 skin samples are used in test step.

In the Table I, the results are presented for different values of K in KNN classifier. As seen, when K increases, the CDR increases as well. For K = 13, the highest CDR is obtained equal to 0.8688. Also, the minimum value of FAR is also obtained for K = 13 which is equal to 0.1201, and K = 11 minimizes the FRR to 0.0100. From these results, we can choose K = 13 to obtain the highest performance of the proposed skin-detector system.

In Fig. 4, detected skin pixels in several images are shown, which demonstrate the efficiency of the proposed skin-detector system.

TABLE I

Performance of proposed skin-detector system

K	CDR	FAR	FRR
1	0.7690	0.2136	0.0174
3	0.8616	0.1214	0.0171
5	0.8623	0.1210	0.0167
7	0.8649	0.1221	0.0130
9	0.8681	0.1206	0.0113
11	0.8687	0.1213	0.0100
13	0.8688	0.1201	0.0111
15	0.8687	0.1203	0.0110
17	0.8681	0.1209	0.0110
19	0.8671	0.1221	0.0109
21	0.8676	0.1211	0.0114

CONCLUSION

A new method was presented in this paper for skin detection in color images based on components of YCbCr and Lab color spaces. Since RGB components are very sensitive to lighting conditions, input image must be transformed to another color space in which light component is separated from other components. C_b and C_r components from YC_bC_r color space and b component from *Lab* color space are chosen to construct primary features. Then, these features are given to SDA and finally optimized features by SDA are given to KNN with K = 13 to distinguish skin pixels from non-skin pixels. Results show that proposed skin-detector has high CDR and low FAR, FRR.

REFERENCES

[1] A.S. Naji, R. Zainuddin, and H.A. Jalab, "Skin segmentation based on multi pixel color clustering model," *Digital Signal Processing*, vol. 22, no. 6, pp. 933-940, 2012.

[2] P. Hiremath and A. Danti, "Detection of multiple faces in an image using skin color information and lines-of-separability face model," *International Journal of Pattern Recognition and Artificial Intelligence*, vol. 20, pp. 39–62, 2006.

[3] L. Wang, W. Hu, and T. Tan, "Recent developments in human motion analysis," *Pattern Recognition*, vol. 36, pp. 585–601, 2003.

[4] X. Zhu, L. Yang, A. Waibel, "Segmenting hands of arbitrary color," in *Proc. of IEEE Int'l Conf. on Automatic Face and Gesture Recognition*, pp. 446-453, 2000.

[5] J.S. Lee, Y.M. Kuo, P.C. Chung, and E. Chen, "Naked image detection based on adaptive and extensible skin color model," *Pattern Recognition*, vol. 40, pp. 2261–2270, 2007.

[6] M. Fleck, D. Forsyth, and C. Bregler, "Finding naked people," in *Proc. of European Conference on Computer Vision*, pp. 592-602, 1996.

[7] C.A. Doukim, J.A. Dargham, and A. Chekima, "Finding the number of hidden neurons for an MLP neural network using coarse to fine search technique," In Proc. *of IEEE Int'l Conf. on Information Sciences Signal Processing and their Applications*, pp. 606-609, 2010.

[8] J. Han, G. Awad, and A. Sutherland, "Automatic skin segmentation and tracking in sign language recognition," *IET Computer Vision*, vol. 3, no. 1, pp. 24-35, 2009.

[9] T.H. Huang, Y.M. Yu, X.G. Qin, "A High-Performance Skin Segmentation Method," *Procedia Engineering*, vol. *15*, pp. 608-612, 2011.

[10] S.L. Phung, D. Chai, and A. Bouzerdoum, "Adaptive skin segmentation in color images," in *Proc. of IEEE Int'l Conf. on Multimedia and Expo*, vol. 3, pp. III-173, 2003.

[11] P. Ng and C.M. Pun, "Skin color segmentation by Texture Feature Extraction and K-mean Clustering," in *Proc. of IEEE Int'l Conf. on Computational Intelligence, Communication Systems and Networks* pp. 213-218, 2011.

[12] M. Jones and J.M. Rehg, "Statistical color models with applications to skin detection," *International Journal of Computer Vision*, vol. 46, pp. 81-96, Jan. 2002.

[13] D. Cai, X. He, J. Han, "Semi-supervised discriminant analysis," in *Proc. of IEEE Int'l Conf. on Computer Vision*, pp. 1-7, 2007.

[14] V. Vezhnevets, V. Sazonov, and A. Andreeva, "A survey on pixel-Based skin color detection technique", in *Proc. of Graphicon*, pp. 85-92. 2003.

[15] J. Yang, W. Lu, and A. Waibel, "Skin-color modeling and adaptation," Springer Berlin Heidelberg, pp. 687-694, 1997.

[16] B. Schauerte and G.A. Fink, "Web-based learning of naturalized color models for human-machine interaction," in *Proc. of IEEE Int'l Conf. on Digital Image Computing: Techniques and Applications*, pp. 498-503, 2010.